PRAMANA
— journal of
physics

Vol. 41, No. 4,
October 1993
pp. 295–309

Controlling of chaos by weak periodic perturbations in Duffing–van der Pol oscillator

S RAJASEKAR
Department of Physics, Manonmaniam Sundaranar University, Tirunelveli 627002, India

MS received 12 April 1993; revised 30 July 1993

Abstract. This paper investigates the possibility of controlling horseshoe and asymptotic chaos in the Duffing–van der Pol oscillator by both periodic parametric perturbation and addition of second periodic force. Using Melnikov method the effect of weak perturbations on horseshoe chaos is studied. Parametric regimes where suppression of horseshoe occurs are predicted. Analytical predictions are demonstrated through direct numerical simulations. Starting from asymptotic chaos we show the recovery of periodic motion for a range of values of amplitude and frequency of the periodic perturbations. Interestingly, suppression of chaos is found in the parametric regimes where the Melnikov function does not change sign.

Keywords. Duffing–van der Pol oscillator; chaos; controlling chaos; Melnikov method.

PACS Nos 05·45; 42·50; 42·65; 47·20

1. Introduction

The genericity and robustness of chaotic dynamics are now well established in typical nonlinear dynamical systems. In recent years, there has been growing interest to use chaos profitably by synchronizing chaotic orbits [1,2] and design of mixing and transport processes [3]. At the same time there have been promising developments in controlling of chaos [4–12]. For example, adaptive control algorithm [5,6], stabilization of unstable periodic orbits embedded in a chaotic attractor by a predetermined perturbation [4] and weak feedback signal [8] have been proposed. Suppression of chaos by weak periodic parametric perturbation [7] and addition of second periodic force [9] are also possible. In fact, shift in the period doubling bifurcations and the onset of chaos due to periodic perturbations have been reported earlier in the literature [13, 14]. In a recent paper, Rajasekar and Lakshmanan [12] numerically studied the applicability and efficacy of various control algorithms in Bonhoeffer–van der Pol oscillator.

In this paper, we investigate, analytically and numerically, the effect of periodic parametric and addition of second periodic force in Duffing–van der Pol (DVP) equation

$$\ddot{x} + p\dot{x}(1 - x^2) - \alpha^2 x + \beta x^3 = f\cos\omega t. \tag{1}$$

The motivation for our interest in this system is that it has wide range of applications in physics and biology. Equation (1) is an alternative form of Bonhoeffer–van der Pol oscillator [11, 12], driven magnetic oscillator [15] and also describes the dynamics of charge density in the plasma of a rf gas discharge. It exhibits well developed chaos in the parameter space [15–18]. Our objective here is to explore the possibility of

controlling the horseshoe dynamics and asymptotic chaos using both analytical and numerical techniques. Horseshoe is the occurrence of transverse intersections of stable and unstable manifolds of saddle fixed point in the Poincaré map and is a global phenomenon [19, 20]. The appearance of which can be predicted analytically using the Melnikov technique [19]. It is well-known that the existence of horseshoe does not imply that the typical trajectories will be asymptotically chaotic. The asymptotically chaotic motion is characterized by positive maximal Lyapunov exponent. In our present analysis we use the Melnikov method to study the influence of periodic perturbations on horseshoe dynamics. Lyapunov exponents and Poincaré map are used to detect the suppression of chaos.

Firstly we investigate the effect of parametric perturbation $\beta\eta x^3 \cos\Omega t$ added in (1). The unperturbed part of the system (1) ($p = f = \eta = 0$) possesses two homoclinic orbits which we denote as W_+ and W_-. For $\eta = 0$ we fixed the value of other parameters at a specific value so that the system shows both asymptotic chaos and transverse intersections of homoclinic orbits. From the Melnikov analysis we found that suppression of horseshoe is not possible in the (η, Ω) parameter space. However, we are able to identify the parametric regimes where intersections of stable and unstable branches of either W_+ or W_- alone occur. On the other hand, suppression of stable chaotic motion is found for range of values of amplitude and frequency of the perturbation. Secondly, we report our analytical and numerical studies on the DVP equation (1) with the second weak periodic force $\eta \cos\Omega(t + \phi)$ where ϕ is the initial phase shift. The most striking result is that horseshoe chaos is suppressed in various regimes in the (η, ϕ) parameter space. These regimes are predicted analytically using the Melnikov method. Analytical prediction is in good agreement with the numerical result. Another key observation is the recovery of periodic behaviour in the parametric intervals where the Melnikov function does not change sign.

The paper is organized as follows. In § 2 chaotic dynamics in DVP equation for a specific parametric choice is briefly reviewed. Then the effect of parametric perturbation on horseshoe dynamics is analysed using the Melnikov method. The analytical prediction is demonstrated through direct numerical simulations. Controlling of asymptotic chaos is also studied. Section 3 is devoted to the detailed study of DVP oscillator driven by second periodic force. Threshold curves in the (η, ϕ) space for the suppression of horseshoe is obtained. The analytical prediction is compared with the numerical results. Further, numerical simulations are performed to study the controlling of asymptotic chaos through maximal Lyapunov exponent. Finally, § 4 contains summary and conclusion.

2. Parametrically driven Duffing–van der Pol oscillator

2.1 *Preliminaries and calculation of Melnikov function*

We consider the DVP equation with a periodic parametric perturbation of the cubic term

$$\dot{x} = y, \tag{2a}$$

$$\dot{y} = \alpha^2 x - \beta x^3(1 + \varepsilon\eta \cos\Omega t) - \varepsilon[p(1 - x^2)y - f\cos\omega t], \tag{2b}$$

where η is the amplitude and Ω the frequency of the periodic perturbation. Because the Melnikov method is based on the perturbation theory we have introduced a small parameter ε into the equations of motion.

The unperturbed system of (2)($\varepsilon = 0$) has a saddle fixed point $(x^*, y^*) = (0, 0)$ and two centre type fixed points $(\pm \alpha/\sqrt{\beta}, 0)$. The two homoclinic orbits which connects saddle to itself are given by

$$W_{\pm}(x_h(\tau), y_h(\tau)) = (\pm \alpha\sqrt{2/\beta}\,\mathrm{sech}\,\alpha\tau,\ \mp \alpha^2\sqrt{2/\beta}\,\mathrm{sech}\,\alpha\tau\,\tanh\alpha\tau),\quad \tau = t - t_0. \tag{3}$$

For $\varepsilon = 0$, the stable and unstable branches of homoclinic orbits join smoothly. When the dissipative perturbation is included the stable manifold W^s and the unstable manifold W^u do not join. However, above certain critical amplitude of the external periodic force, transverse intersections of W^s and W^u occur. The presence of such intersections implies that the Poincaré map has the so-called horseshoe chaos [19, 20]. Even though the orbits created by the horseshoe mechanism are unstable they can exert a dramatic influence on the behaviour of orbits which pass close to the point of intersection. These orbits will display an extremely sensitive dependence on initial conditions and exhibit a chaotic transient before settling to a periodic or strange attractors. The appearance of transverse intersections of homoclinic orbits can be predicted analytically by the Melnikov technique. For a system of the form

$$\mathrm{d}X/\mathrm{d}t = h_0(X) + \varepsilon h_1(X, t, \varepsilon), \tag{4}$$

where $X = (x, y)$, $h_0 = (f_0, g_0)$ and $h_1 = (f_1, g_1)$ the expression for the Melnikov function is given by [19, 20]

$$M(t_0) = \int_{-\infty}^{\infty} h_0(X_h(\tau)) \wedge h_1(X_h(\tau), t) \exp\left[-\int_0^{\tau} \mathrm{trace}[D_X(h_0(X_h(s)))]\,\mathrm{d}s \right] \mathrm{d}\tau. \tag{5}$$

Here X_h represents homoclinic orbit, $h_0 \wedge h_1 = f_0 g_1 - f_1 g_0$ and D_X denotes the partial derivative with respect to X.

For the DVP equation (2) the Melnikov function is

$$M(t_0) = \int_{-\infty}^{\infty} y_h[-p y_h(1 - x_h^2) - \beta\eta x_h^3 \cos\Omega(\tau + t_0) + f\cos\omega(\tau + t_0)]\mathrm{d}\tau. \tag{6}$$

Evaluating the integral using (3) we obtain

$$M(t_0) = \pm Af \sin\omega t_0 - B\eta \sin\Omega t_0 - C, \tag{7a}$$

where

$$A = \sqrt{2/\beta}\pi\omega\,\mathrm{sech}(\pi\omega/(2\alpha)),$$

$$B = (\pi/(6\beta))\Omega^2(4\alpha^2 + \Omega^2)\mathrm{cosech}(\pi\Omega/(2\alpha)),$$

$$C = 4p\alpha^3(5\beta - 4\alpha^2)/(15\beta^2). \tag{7b}$$

Before we go on to study the effect of parametric perturbation we briefly show the occurrence of chaotic dynamics for $\eta = 0$. For $\eta = 0$, the condition for transverse intersection of W^s and W^u is that $M(t_0)$ changes sign at some t_0 which occurs, from (7), for

$$|f| \geq f_M = 2\sqrt{2}p\alpha^3(5\beta - 4\alpha^2)\cosh(\pi\omega/(2\alpha))/(15\beta^{3/2}\pi\omega). \tag{8}$$

Equation (8) is the necessary condition for the occurrence of horseshoe. The sufficient condition requires the existence of simple zeros of $M(t_0)$. For our further analysis we fix $\alpha = 1$, $\beta = 5$ and $p = 0{\cdot}4$. For $\omega = 1$ the Melnikov analytical threshold value f_M is 0·1132. Figure 1 shows the numerically computed W^s and W^u of the saddle in the Poincaré map for $f = 0{\cdot}08$ and $f = 0{\cdot}125$. The unstable manifolds are obtained by integrating eq. (2) in the forward time for a set of 200 initial conditions chosen around the perturbed saddle point. The stable mainfolds are obtained by integrating the equations of motion in reverse time. For $f = 0{\cdot}08$ the two orbits are separated for which the Melnikov function is always negative. For $f = 0{\cdot}125$ from figure 1b we can clearly notice transverse intersections of orbits at four places. For $f < 0{\cdot}125$ asymptotically periodic motion is observed. Onset of chaotic motion is observed at $f = 0{\cdot}125$. For clarity, the chaotic orbit in the $x - y$ plane and the strange attractor

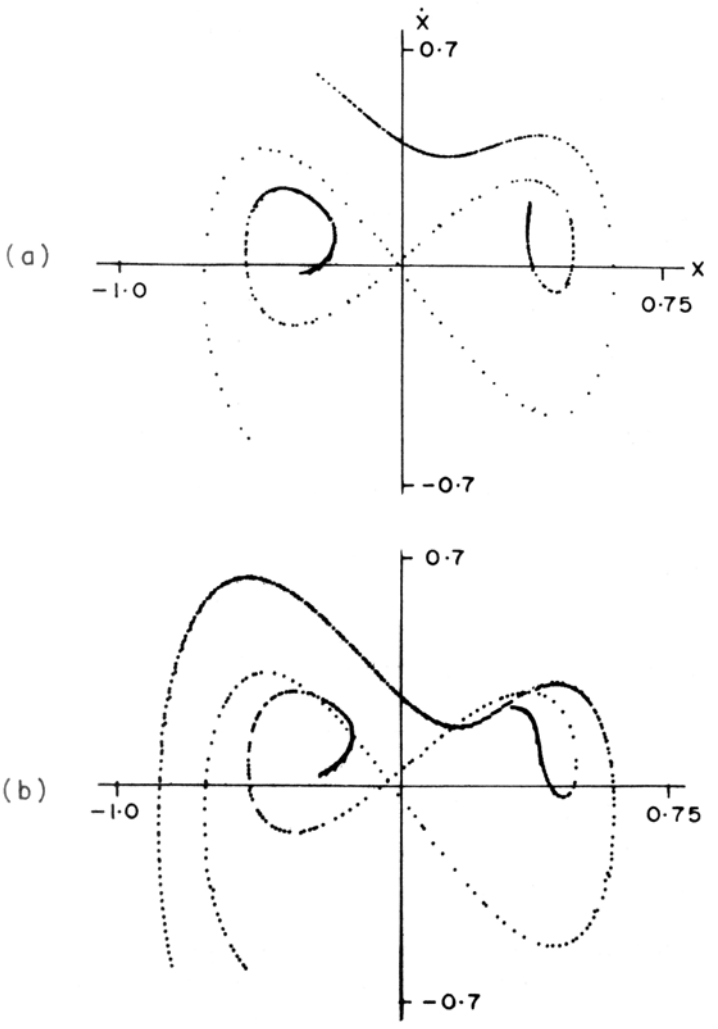

Figure 1. Numerically computed stable and unstable manifolds of saddle fixed point for $\alpha^2 = 1$, $\beta = 5$, $\omega = 1$, $\eta = 0$ and (**a**) $f = 0{\cdot}08$ and (**b**) $f = 0{\cdot}125$.

in the Poincare map are given in figure 2. We also study the effect of periodic perturbations on horseshoe dynamics and chaotic motion observed for $f = 0{\cdot}125$.

2.2 *Effect of weak parametric perturbation on homoclinic bifurcation*

For $\eta \neq 0$ the necessary condition for $M(t_0)$ to change sign is

$$\eta^{\pm} \leqslant \eta_M = \frac{6\beta(\pm Af - C)\sinh(\pi\Omega/2\alpha)}{\pi\Omega^2(4\alpha^2 + \Omega^2)}, \tag{9a}$$

or

$$\eta^{\pm} \geqslant \eta_M = \frac{6\beta(\pm Af + C)\sinh(\pi\Omega/2\alpha)}{\pi\Omega^2(4\alpha^2 + \Omega^2)}, \tag{9b}$$

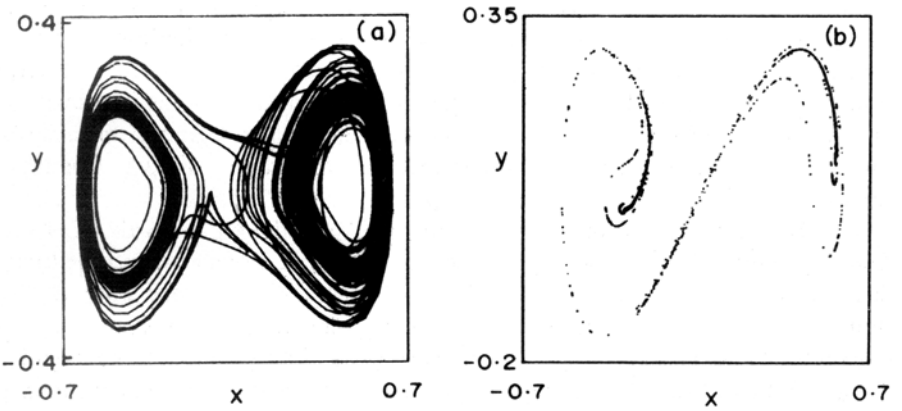

Figure 2. (**a**) Phase portrait and (**b**) Poincaré map of the chaotic attractor for $f = 0{\cdot}125$.

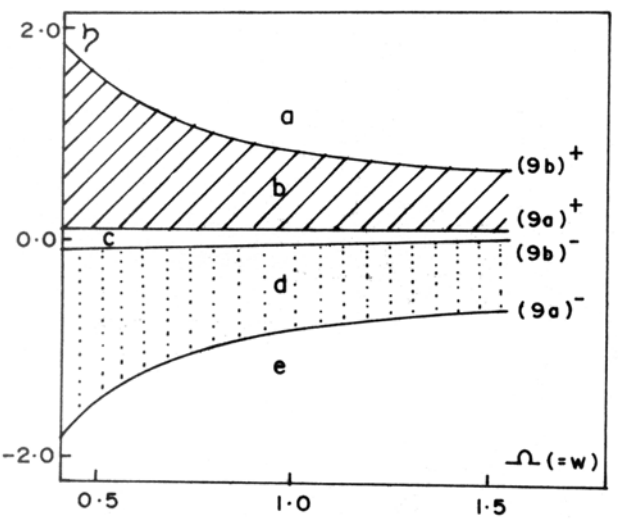

Figure 3. Melnikov threshold curves for horseshoe chaos in (η, Ω) plane.

where the superscripts '+' and '−' refer to the homoclinic orbits W_+ and W_- respectively. In general, for arbitrary values of ω and Ω, the above condition is not sufficient to ensure the existence of simple zeros of $M(t_0)$ in (7). However, the condition (9) is sufficient if the frequency Ω is in resonance with ω, that is, $p\Omega = q\omega$ where p and q are some positive integers. Figure 3 shows the threshold value of $\eta(\Omega)$ for $\Omega = \omega$. In the (η, Ω) parameter space tranverse intersections of W^s_+ and W^u_+ occur below the curve $(9a)^+$ and above the curve $(9b)^+$. While one can expect transverse intersections of W^s_- and W^u_- above the curve $(9b)^-$ and below the curve $(9a)^-$. Thus, horseshoe chaos occur in the entire (η, Ω) parameter space. However, in the shaded (dotted) region intersections of stable and unstable branches of $W_+ (W_-)$ do not occur. We have verified the above analytical predictions by direct numerical simulations of the DVP equation (2). As an example, figure 4 shows the part of the stable and unstable orbits of saddle in the Poincaré map for $\Omega = 1$ and for four values of η chosen in the regions, *a*, *b*, *c* and *d*. Transverse intersections of stable and unstable branches of both the homoclinic orbits W_+ and W_- can be clearly seen in figure 4a for $\eta = 0{\cdot}85$ which falls in the region *a*. In figure 4b we see the intersections of W_- orbits alone at one place for $\eta = 0{\cdot}3$ (region *b*). While for $\eta = -0{\cdot}01$ (region *c*) intersections of both the homoclinic orbits has been found. This is shown in figure 4c. For $\eta = -0{\cdot}25$ (figure 4d), which correspond to the region *d*, branches of W_+ orbit alone found to intersect. These numerical results agree well with the theoretical predictions.

For $\Omega \neq \omega$ the appearance of horseshoe can be studied numerically measuring the time τ_M elapsed between two successive transverse intersections. τ_M, the first simple zero of $M(t_0)$, can be determined from (7). In figure 5 we have plotted $1/\tau_M$ as a function of Ω for $\eta = 0{\cdot}02$. Curve *a* corresponds to positive sign while curve *b* corresponds to negative sign in (7). Horseshoe chaos occur in the region where $1/\tau_M > 0$. Lower the $1/\tau_M$, higher is the number of iterates of Poincare map needed to guarantee a horseshoe. When Ω increases new intersection times suddenly appear which are responsible for the observed jumps of the function $1/\tau_M$ in figure 5. Further, we note that for Ω less than certain critical value the $1/\tau_M$ depicted by the curve *a* becomes zero, which indicates that in this Ω interval intersection of orbits of W_+ does not occur.

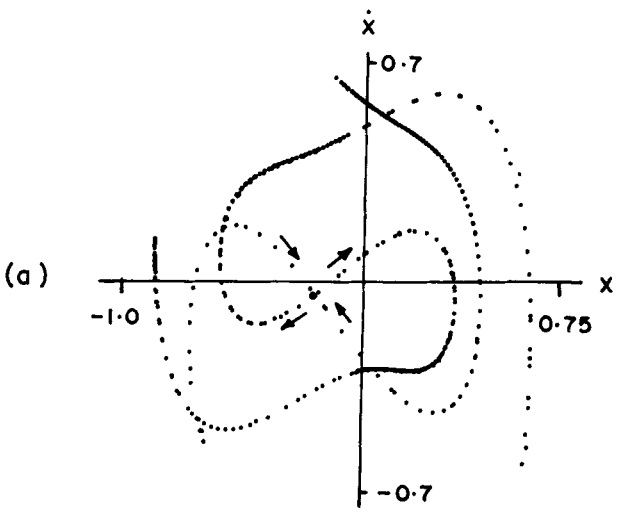

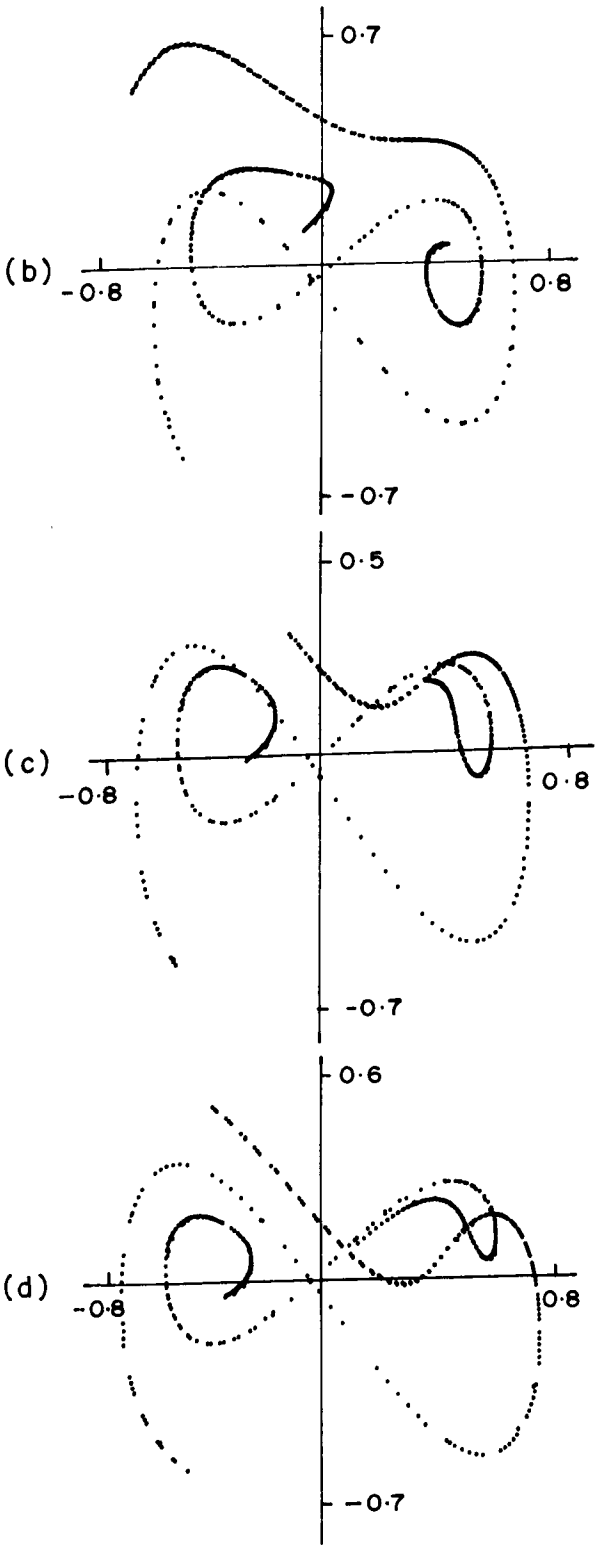

Figure 4. Parts of the stable and unstable manifolds of the saddle fixed point in the Poincaré map of (2) for (**a**) $\eta = 0{\cdot}85$, (**b**) $\eta = 0{\cdot}3$, (**c**) $\eta = -0{\cdot}01$ and (**d**) $\eta = -0{\cdot}25$.

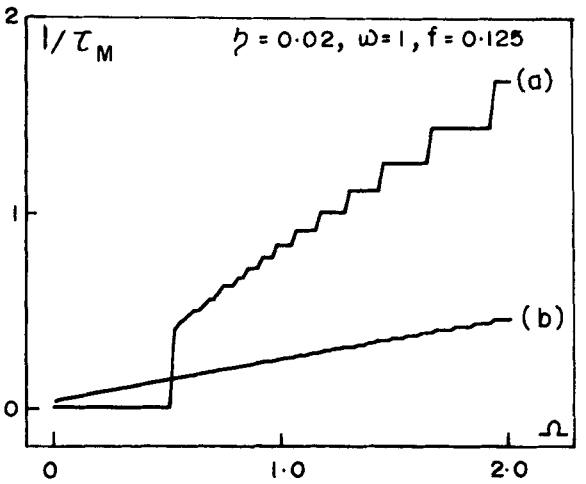

Figure 5. Variation of $1/\tau_M$ versus Ω for $\eta = 0{\cdot}02$. Curve a is for positive sign and curve b is for negative sign in equation (7).

2.3 *Controlling of asymptotic chaos*

In this subsection, starting from a chaotic region (figure 2) we explore the possibility of suppression of chaos for a range of values of η and Ω. A full-fledged phase diagram would be very valuable; however, with the limited computing facilities available we have investigated the dynamics in a restricted region, namely, (i) Ω fixed and η varying with increment $\Delta\eta = 0{\cdot}005$, (ii) η fixed and Ω varying with $\Delta\Omega = 0{\cdot}01$.

We confine our analysis in the parameter regime $\eta \in (0, 0{\cdot}2)$ and $\Omega \in (0, 3)$ only. For $\Omega = 0{\cdot}5$ chaotic behaviour persists for $\eta \leqslant 0{\cdot}13$ and period-$2T(T = 2\pi/\omega)$ motion is observed for $\eta \geqslant 0{\cdot}135$. For $\Omega = 1$ and 2 periodic motion with period-T occurs for $\eta \geqslant 0{\cdot}005$. Regular motion is recovered for Ω values near the resonance value to ω. For example, when $\Omega = 1{\cdot}1$ period $-10T$ orbit is found for η values in the interval (0·055, 0·065), (0·085, 0·105) and (0·115, 0·2). Similarly, for fixed η values the nature of orbits for different Ω has been investigated. For small values of η regular motion is observed for very narrow regimes of Ω values. For $\eta = 0{\cdot}05$ periodic motion is found only at $\Omega = 1{\cdot}0(p-1)$, $2(p-1)$ and $3(p-4)$ and for $\eta = 0{\cdot}1$ suppression of chaotic behaviour is observed at $\Omega = 1(p-1)$, $1{\cdot}1(p-10)$ and $2(p-1)$. However, the width of the regular regime increases with increase in η. For example, for $\eta = 0{\cdot}18$ periodic motion is recovered at $\Omega = 0{\cdot}5(p-2)$, $0{\cdot}8(p-5)$, $1{\cdot}0(p-1)$, $1{\cdot}6(p-5)$, $1{\cdot}7(p-10)$, $1{\cdot}8(p-5)$, $2{\cdot}0(p-1)$, $2{\cdot}2(p-10)$, $2{\cdot}4(p-5)$, $2{\cdot}5(p-5)$, $2{\cdot}8(p-5)$ and $3(p-1)$.

3. Effect of second periodic force

One can also control the dynamics of a system by the addition of an external weak periodic force in the chaotic state. The DVP equation with second periodic force can be written as

$$\dot{x} = y, \tag{10a}$$

$$\dot{y} = \alpha^2 x - \beta x^3 - \varepsilon[p(1-x^2)y - f\cos\omega t - \eta\cos\Omega(t+\phi)], \tag{10b}$$

where ϕ is the phase shift. Here again we investigate controlling of chaotic dynamics using both Melnikov method and numerical techniques.

3.1 *Suppression of horseshoe chaos*

For system (10) the Melnikov function works out to be

$$M(t_0) = \pm Af \sin \omega t_0 \pm B\eta \sin \Omega(t_0 + \phi) - C, \tag{11a}$$

where

$$A = \sqrt{2/\beta}\pi\omega \operatorname{sech}(\pi\omega/2\alpha), \quad B = \sqrt{2/\beta}\pi\Omega \operatorname{sech}(\pi\Omega/2\alpha),$$
$$C = 4p\alpha^3(5\beta - 4\alpha^2)/(15\beta^2). \tag{11b}$$

First, we consider the case where the phase shift ϕ is zero. Now $M(t_0)$ becomes

$$M(t_0) = \pm Af \sin \omega t_0 \pm B\eta \sin \Omega t_0 - C. \tag{12}$$

Since the choice $\Omega = \omega$ is trivial we study the existence of horseshoe for $\Omega \neq \omega$. As mentioned earlier, we cannot write the Melnikov condition similar to (9) for arbitrary values of ω and Ω. So, we estimate the first intersection time τ_M and identify the parametric regime where $1/\tau_M \approx 0$. Figure 6 shows the plot of $1/\tau_M$ against Ω for $\eta = -0{\cdot}2$, $\omega = 1$ and $f = 0{\cdot}125$. Curve *a* represents the inverse of first intersection time of stable and unstable branches of the homoclinic orbit W_+. Curve *b* corresponds to the orbit W_-. $1/\tau_M$ is nonzero for the whole interval of Ω except at $\Omega = 1$. At $\Omega = 1$, $1/\tau_M$ is zero. This implies that horseshoe does not occur at $\Omega = 1$.

Now we describe what happens when ϕ is not zero. For $\phi > 0$ and $\omega = \Omega$ (which gives $A = B$) the Melnikov function is given by

$$M(t_0) = \pm(Af + A\eta \cos \omega\phi) \sin \omega t_0 \pm A\eta \sin \Omega\phi \cos \omega t_0 - C. \tag{13}$$

From the above equation, the condition for $M(t_0)$ to change sign is

$$\eta^2 + 2\eta \cos \Omega\phi + (f^2 - C^2/A^2) \geqslant 0. \tag{14}$$

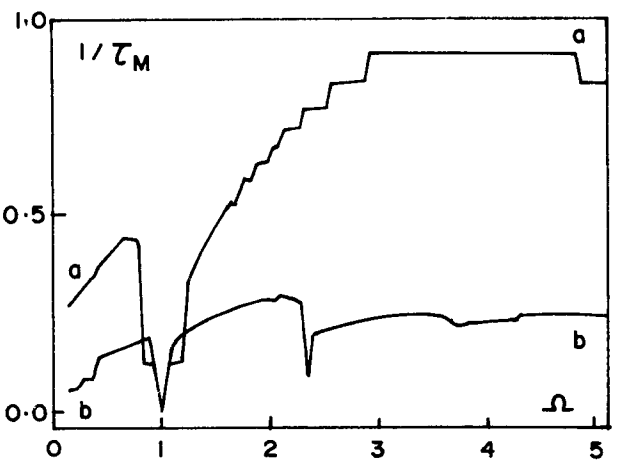

Figure 6. $1/\tau_M$ versus Ω for $\eta = -0{\cdot}2$. Curve *a* corresponds to positive sign while curve *b* corresponds to negative sign in equation (12).

When the equality is satisfied we have

$$\eta = -\cos\Omega\phi \pm [f^2\cos^2\Omega\phi + (C^2/A^2 - f^2)]^{1/2}. \qquad (15)^{\pm}$$

From (14) and (15) we note that $M(t_0)$ changes sign, that is, the transverse intersection of homoclinic orbits, occur above and below the curves given by equations $(15)^+$ and $(15)^-$ respectively. These curves are shown in figure 7 for $\Omega = 1$. In the parametric regions *a*, *b* and *c* enclosed by the curves, $M(t_0)$ does not change sign and hence transverse intersections of homoclinic orbits do not occur. This is exactly what we observed numerically. As an example, figure 8 shows the numerical simulations for three η values. We fixed the value of ϕ at 1·0. For this choice from (14) we note that $M(t_0)$ changes sign and transverses intersections of homoclinic orbits occur for $\eta > -0{\cdot}026$ and $\eta < -0{\cdot}11$. This is shown in figures 8a and 8c for $\eta = -0{\cdot}02$ and $-0{\cdot}13$ respectively. Further, one can expect suppression of transverse intersections of orbits for $\eta \in (-0{\cdot}11, -0{\cdot}026)$. This is depicted in figure 8b for $\eta = -0{\cdot}05$ where both the orbits are well separated. Thus, suppression of horseshoe can be achieved for a range of values of η, Ω and ϕ.

3.2 *Controlling of asymptotic chaos*

Now we show the suppression of chaotic motion depicted in figure 2 by second periodic force. We have carried out analysis for Ω fixed and η varying with $\Delta\eta = 0{\cdot}005$. Table 1 summarizes the behaviour of the system as a function of the parameter η for five fixed values of Ω with $\phi = 0$. From this table we note that regular motion can be recovered for wide range of values of η and Ω. Here the suppression of chaos is by mode-locking.

Next, we consider the case $\phi > 0$. We have pointed out earlier that the Melnikov function $M(t_0)$ does not change sign and consequently no horseshoe dynamics occur in the regions *a*, *b* and *c* of figure 7. The striking result is that suppression of stable

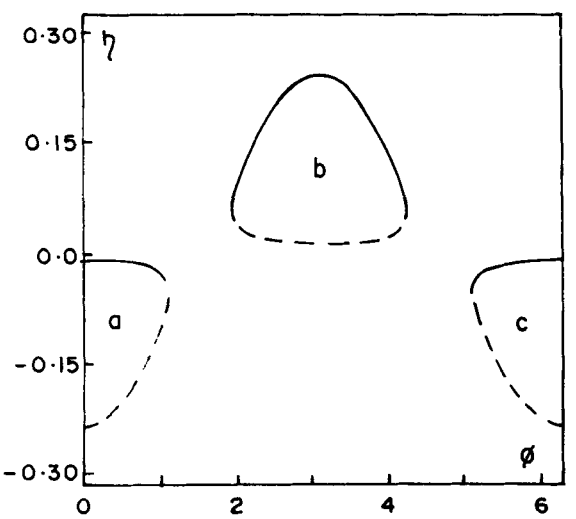

Figure 7. Graph of $(15)^{\pm}$. Horseshoe does not occur in the regions *a*, *b* and *c* enclosed by the curves. Continuous and dashed curves represent the solution of equation $(15)^+$ and equation $(15)^-$ respectively.

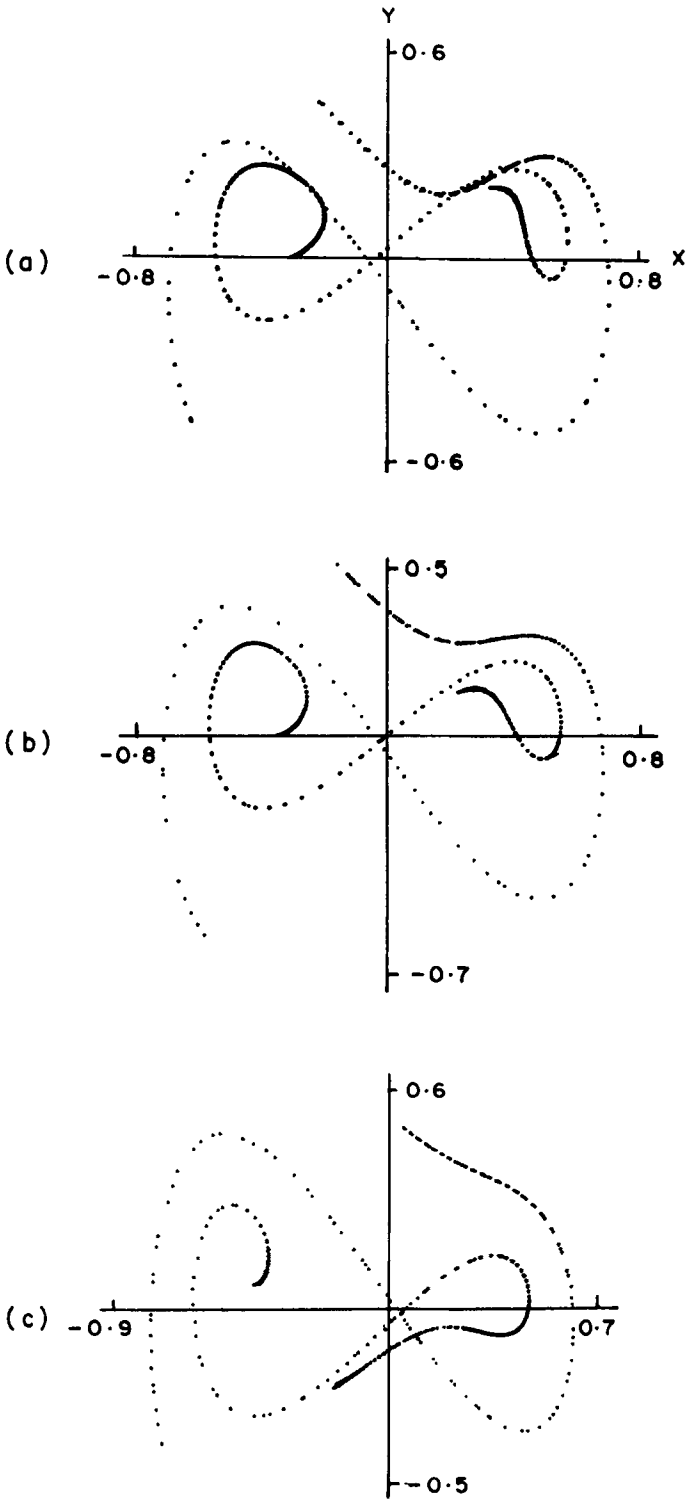

Figure 8. Numerically computed part of perturbed homoclinic orbits for (**a**) $\eta = -0{\cdot}02$, (**b**) $\eta = -0{\cdot}05$ and (**c**) $\eta = -0{\cdot}13$. The other parameters in equation (10) are fixed at $\alpha^2 = 1$, $\beta = 5$, $\omega = 1$, $f = 0{\cdot}125$, $\Omega = 1$ and $\phi = 1$.

Table 1. Dynamical behaviour of the DVP equation in the presence of second periodic force for five fixed values of Ω as a function of η.

Ω	η	behaviour
0·5	0 – 0·045	chaos
	0·05	period-6
	0·055 – 0·2	period-2
1·0	0 – 0·135	chaos
	0·14 – 0·2	period-1
1·4	0 – 0·045	chaos
	0·05 – 0·18	period-5
	0·185 – 0·2	chaos
1·5	0 – 0·08	chaos
	0·085 – 0·175	period-5
	0·18 – 0·19	period-8
2·0	0	chaos
	0·005 – 0·165	period-1
	0·17 – 0·2	chaos

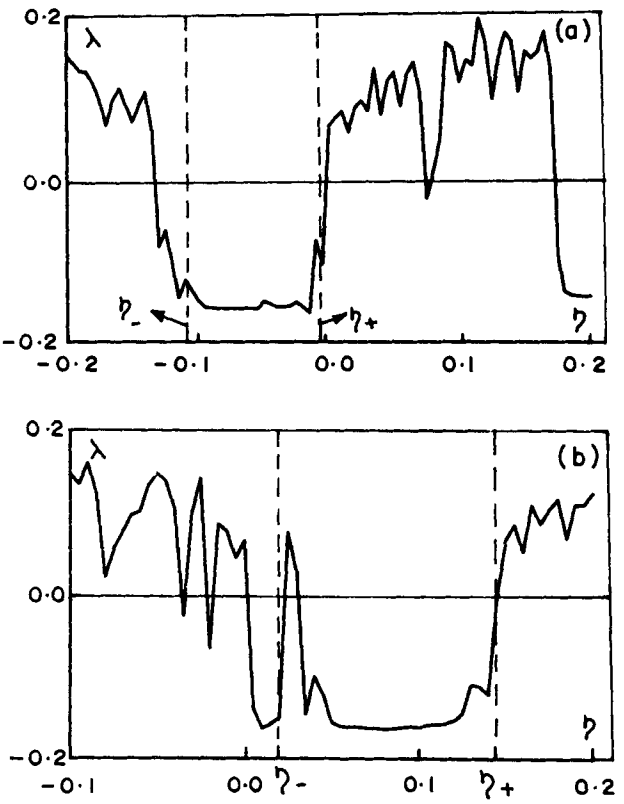

Figure 9. Estimated maximal Lyapunov exponent versus the parameter η for (**a**) $\phi = 1$ and (**b**) $\phi = 2{\cdot}2$. η_+ and η_- are the Melnikov threshold values given by the equation $(15)^{\pm}$.

chaotic motion is also found in these parametric regions. In figure 9 maximal Lyapunov exponent (λ) versus the parameter η is reported for $\Omega = 1$, $\phi = 1$ and 2·2. For $\phi = 1$ as shown earlier transverse intersections of homoclinic orbits do not occur for η values in the interval $(-0{\cdot}11, -0{\cdot}026)$. From figure 9a we find that λ is negative for $\eta \in (-0{\cdot}13, -0{\cdot}005)$. Similar result has been observed for various ϕ values in the regions *a*, *b* and *c*. For clarity, we summarize our results in table 2 for two values of ϕ. From our detailed analysis we infer that the Melnikov function $M(t_0)$ does not change sign for all t_0. This can serve as an analytical criterion to study the suppression of asymptotic chaos.

We have also performed our analysis outside the regions *a*, *b* and *c* of figure 7. In these regions horseshoe still persists. However, it is well known that the presence of horseshoe does not guarantee that typical long time motion is chaotic. In fact, in these regions we found regular behaviour for very narrow ranges of η and Ω values. This is evident from figure 10 where λ is negative only at six narrow ranges of η

Table 2. Details of theoretical and numerical predictions of the DVP system with second periodic force. $M(t_0)$ and λ denote the Melnikov function and maximal Lyapunov exponent respectively.

ϕ	η interval where the sign of $M(t_0)$ remain unchanged	η interval with $\lambda < 0$	η values	behaviour
1·0	$(-0{\cdot}11, -0{\cdot}026)$	$(-0{\cdot}13, -0{\cdot}02)$	$(-0{\cdot}2) - (-0{\cdot}13)$	chaos
			$(-0{\cdot}125) - (-0{\cdot}1)$	period-1
			$(-0{\cdot}095) - (-0{\cdot}03)$	period-2
			$(-0{\cdot}025) - (-0{\cdot}005)$	period-1
			$(0{\cdot}0) - (0{\cdot}2)$	chaos
2·2	$(0{\cdot}022, 0{\cdot}124)$	$(0{\cdot}005, 0{\cdot}02)$,	$(-0{\cdot}1) - (0{\cdot}0)$	chaos
		$(0{\cdot}035, 0{\cdot}145)$	$0{\cdot}005 - 0{\cdot}02$	period-1
			$0{\cdot}025 - 0{\cdot}03$	chaos
			$0{\cdot}035 - 0{\cdot}045$	period-2
			$0{\cdot}05 - 0{\cdot}145$	period-1
			$0{\cdot}15 - 0{\cdot}2$	chaos

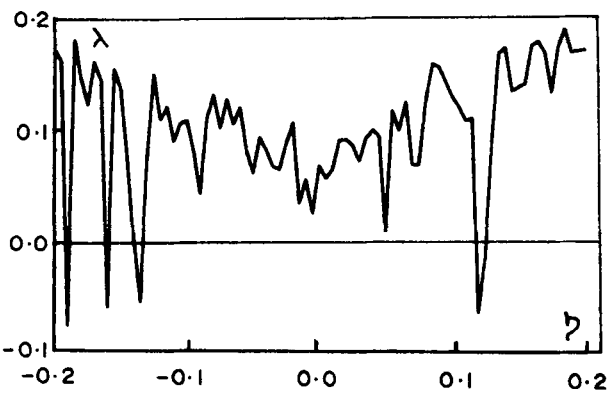

Figure 10. Variation of maximal Lyapunov exponent as a function of the parameter η for $\phi = 1{\cdot}5$.

values for $\phi = 1{\cdot}5$. For example, attractors with period-2 at $\eta = -0{\cdot}19$ and period-3 at $\eta = -0{\cdot}16$, $-0{\cdot}14$, $-0{\cdot}135$, $0{\cdot}12$ and $0{\cdot}125$ are found to occur.

The results presented in this section have shown how a relatively weak periodic force can change the global and local dynamics of the system in a drastic fashion; horseshoe and chaotic dynamics can be controlled.

4. Summary and conclusion

We have studied the effect of periodic perturbations on chaotic dynamics in the DVP oscillator. For typical parametric values we have shown that suppression of horseshoe is not possible by periodic parametric perturbation. However, suppression of horseshoe has been found for a range of amplitude of a second periodic force and phase shift between the two external forces. The system dynamics is sensitive to the initial phase shift. The effect of both types of periodic perturbations on stable chaotic motion is similar. In both the cases regular behaviour has been recovered for range of amplitude and frequency of the weak perturbations.

The other control mechanisms such as adaptive control algorithm [5, 6, 12], Ott-Grebogi-Yorke method [4] and feedback control mechanism [8] have the advantage of stabilizing a desired periodic motion. Whereas our analysis shows that chaotic motion can be converted to some regular motion by weak periodic perturbations. Further, the period of the controlled motion depends on η and Ω values. Thus, for a given chaotic system one has to carry out detailed numerical simulations in η, Ω space to identify the regular regime. However, for the DVP equation we have shown that most of the regular regime can be identified by the Melnikov method. With the good agreement obtained between theoretical and numerical predictions we emphasize that Melnikov analysis can be successfully used to predict the effect of weak periodic perturbations on chaos. In fact, for a large class of physical problems the calculation of Melnikov function is possible and hence the study of controlling of chaos by this analytical method will be of much interest.

Acknowledgements

It is a pleasure to thank Dr K P N Murthy for a critical reading of the manuscript. The author is indebted to Indira Gandhi Centre for Atomic Research, Kalpakkam for a visiting scientist fellowship.

References

[1] L M Pecora and T L Carroll, *Phys. Rev. Lett.* **64**, 821 (1990)
[2] M de Sousa Vieira, A J Lichtenberg and M A Lieberman, *Int. J. Bifur. Chaos* **1**, 691 (1991)
[3] J M Ottino *et al*, *Science* **257**, 754 (1992)
[4] E Ott, C Grebogi and J Yorke, *Phys. Rev. Lett.* **64**, 1196 (1990)
[5] B A Huberman and E Lumer, *IEEE Trans. Circuits Syst.* **37**, 547 (1990)
[6] S Sinha, R Ramaswamy and J Subba Rao, *Physica* **D43**, 118 (1990)
[7] R Lima and M Pettini, *Phys. Rev.* **A41**, 726 (1990)
[8] J Singer, Y Z Wang and H H Bau, *Phys. Rev. Lett.* **66**, 1123 (1991)
[9] Y Braiman and I Goldhirsch, *Phys. Rev. Lett.* **66**, 2545 (1991)
[10] E A Jackson, *Phys. Rev.* **A44**, 4839 (1991)
[11] S Rajasekar and M Lakshmanan, *Int. J. Bifur. Chaos* **2**, 201 (1992)
[12] S Rajasekar and M Lakshmanan, *Physica* **D67** 282 (1993)

[13] K Wiesenfeld and B McNamara, *Phys. Rev.* **A33**, 629 (1986)
[14] P Bryant and K Wiesenfeld, *Phys. Rev.* **A33** 2525 (1986)
[15] J Fang, *Phys. Lett.* **A146**, 35 (1990)
[16] S Rajasekar, S Parthasarathy and M Lakshmanan, *Chaos, Solitons and Fractals* **2**, 271 (1992)
[17] G P King and S T Gaito, *Phys. Rev.* **A46** 3092 (1992)
[18] M G M Gomes and G P King, *Phys. Rev.* **A46** 3100 (1992)
[19] S Wiggins, *Global bifurcations and chaos* (Springer, Berlin, 1988)
[20] J Guckenheimer and P Holmes, *Nonlinear oscillations, dynamical systems and vector fields* (Springer, Berlin, 1983)